IOP Publishing Journal of Physics: Condensed Matter
J. Phys.: Condens. Matter **26** (2014) 426001 (11pp) doi:10.1088/0953-8984/26/42/426001

Relation between spin and orbital magnetism in excited states of ferromagnetic materials

L M Sandratskii

Max-Planck-Institut für Mikrostrukturphysik, Weinberg 2, 06120 Halle, Germany

E-mail: lsandr@mpi-halle.mpg.de

Received 16 June 2014, revised 18 August 2014
Accepted for publication 1 September 2014
Published 2 October 2014

Abstract

We report the first-principles study of the orbital magnetism, the magnetic anisotropy energy, the ratio of the spin, and the orbital moments in nano-sized systems perturbed from their magnetic ground state. We investigate one monolayer thick films of Co, Fe, and FePt. Two types of the perturbation are studied. First, the collinear spin structure is rotated continuously between the easy and hard axes. Second, the non-collinear spin structures are considered varying in both the angles between spin moments and the direction of the net magnetization. In agreement with the experiment we obtain a variety of behaviours. We show that the magnetic anisotropy energy can both increase and decrease with increasing magnetic disorder. The type of behaviour depends on the variation of the electronic structure with increasing angles between atomic moments. We obtain the effect of band narrowing accompanying the spin disorder that correlates with the band narrowing obtained experimentally in a laser irradiated system. In agreement with this experiment we show that the ratio of the spin and orbital moments can both remain unchanged and vary strongly. We analyse the applicability of Bruno's picture, which suggests proportionality between magnetic-anisotropy energy and orbital moment anisotropy for non-collinear spin configurations. We study the non-collinearity of the atomic spin and orbital moments and demonstrate that the response of the orbital moments to the variation of the spin structure can be unexpected and spectacular.

Keywords: spin and orbital magnetism, non-collinear magnetism, excited states

(Some figures may appear in colour only in the online journal)

1. Introduction

Orbital magnetism is a fundamental property of magnetic materials. There are many aspects of modern research that make necessary further advances in the understanding of orbital magnetism. To mention just a few of these factors; first, in the nano-scaled systems that are the focus of modern physics and technology, the atomic orbital moments are strongly enhanced [1–3]. Second, the modern methods of x-ray magnetic circular dichroism spectroscopy (XMCDS) are able to disentangle spin and orbital moments [4–6], which opens up an avenue for a deeper insight into the microscopic properties of magnetic materials. Third, in the ultra-fast processes studied within pump-probe experiments, orbital magnetism plays an important role as a possible channel of angular-momentum dissipation [7]. We should also mention a widely recognized connection between orbital magnetism and magnetic anisotropy, which is the property of the highest practical importance for all types of magnetic devices [5, 8].

In this paper we report a first-principles study of the relation between the spin and the orbital magnetism in the excited states of a number of nano-scaled materials. A typical first-principles study of orbital magnetism is restricted to an evaluation of the orbital moments for the ferromagnetic configurations of atomic spins directed parallel to one of the high symmetry crystallographic axes [9–14].

This is clearly insufficient to address the questions raised by finite-temperature experiments or experiments on laser-irradiated samples. For instance, one of the most challenging problems of the magnetism of itinerant-electron systems is the understanding of the diversity of the temperature dependence of magnetic anisotropy [15–18]. The experiments show the possibility of both an increase and decrease in magnetic anisotropy with increasing temperature, whereas the expected behaviour is a decrease [19].

An interesting example of a modern study of the relation between spin and orbital magnetism is the pump-probe experiment of Boeglin *et al* [6] with the use of XMCDS to probe the system excited by an ultra-short optical pulse. Boeglin's *et al* measurements gave a significant time dependence of the ratio m_{oz}/m_{sz} of the projections of the orbital and spin moments of Co atoms on the normal of a CoPd film during the relaxation process after laser irradiation. On this basis the authors draw their conclusion about the separate dynamics of spin and orbital moments. There is one important aspect that must be investigated before such a conclusion can be drawn: Does the time dependence of the ratio m_{oz}/m_{sz} necessarily mean that the orbital moment constitutes an additional degree of freedom, or that this dependence may be the consequence of a change in the spin structure? We remark that the ratio of the spin and orbital moments was addressed in a number of other experiments and revealed a variety of behaviours [20–23]. The first-principles study of the dependence of the ratio m_{oz}/m_{sz} on the variation of the spin structure was never performed.

The aim of this paper is to gain a deeper insight into the relation between spin and orbital magnetism by means of the consideration of the systems perturbed from their magnetic ground state. In the first-principles calculations we employ the augmented spherical wave (ASW) method generalized for the case of non-collinear magnetic structures and taking into account the spin–orbit coupling (SOC) [25]. The first results of our work in this direction were briefly presented in a recent publication [24]. In the given paper we extend and deepen our study. We begin with a discussion of the microscopic mechanism of the formation of the orbital moment. This lays the foundation for an analysis of the results of the calculations. Then we deal with collinear spin configurations that assume different directions with respect to crystallographic axes. Next, we study the properties of the orbital moments in non-collinear spin configurations. For constrained spin configurations we perform a self-consistent calculation of the electronic structure and evaluate the values and directions of the atomic orbital moments that, in general, are non-collinear to the corresponding atomic spin moments.

2. Calculational approach

Our study is based on the first-principles calculations within the framework of the density functional theory (DFT). In the DFT calculations the specification of the magnetic state is usually made by the information on the directions of the atomic spin moments, whereas the atomic orbital moments appear to be determined by the spin structure. In our calculations the atomic spin and orbital moments are considered as 3D quantities [25] calculated as:

$$m^i_{s\alpha} = \sum_{\mathbf{k}n,\varepsilon^n_{\mathbf{k}}<E} \int_{\Omega_i} \psi^{n+}_{\mathbf{k}}(\mathbf{r})\sigma_\alpha \psi^n_{\mathbf{k}}(\mathbf{r})\mathrm{d}\mathbf{r}, \quad \alpha = x, y, z, \tag{1}$$

$$m^i_{o\alpha} = \sum_{\mathbf{k}n,\varepsilon^n_{\mathbf{k}}<E} \int_{\Omega_i} \psi^{n+}_{\mathbf{k}}(\mathbf{r})\hat{l}_\alpha \psi^n_{\mathbf{k}}(\mathbf{r})\mathrm{d}\mathbf{r}, \quad \alpha = x, y, z, \tag{2}$$

where $\sigma_x, \sigma_y, \sigma_z$ are the Pauli matrices, $\hat{l}_x, \hat{l}_y, \hat{l}_z$ are the operators of the components of the orbital angular momentum, n is the band index and the integration carried out over the ith atomic sphere, $\psi^n_{\mathbf{k}}$ are the spinor wave functions, and $\varepsilon^n_{\mathbf{k}}$ the energies of the electron states. Energy parameter E governs the filling of the electronic bands. The actual value of the moment corresponds to E equal to the Fermi energy. By varying E one can study the effects of different band filling. Local spin density approximation (LSDA) to the exchange-correlation functional [26] was used. For each spin configuration a self-consistent calculation was performed for one orientation of the spin moments with respect to the crystallographic axes. The potentials thus obtained were used to evaluate the band energies of various orientations of this spin configuration with respect to the crystallographic axes and, in this way, to estimate the magnetic anisotropy energy.

The ASW method uses an atomic basis set that employs the spherical harmonics for a description of the angular dependencies. For the projection of the orbital moment on axis η, used in the definition of the spherical harmonics as a polar axis, one obtains a very useful and physically transparent expression[1]:

$$m_{o\eta} = \sum_{m\sigma} m\, n_{m\sigma} = \sum_{(m>0),\sigma} m(n_{m\sigma} - n_{(-m)\sigma}) \tag{3}$$

where $n_{m\sigma}$ is the occupation number for the atomic orbital with magnetic quantum number m and spin projection σ.

In this paper, we will devote our attention to the relation between magnetic anisotropy energy (MAE) and orbital moment anisotropy (OMA) defined as:

$$\mathrm{OMA} = m_o([0\,0\,1]) - m_o([1\,0\,0]),$$
$$\mathrm{MAE} = E_{\mathrm{tot}}([0\,0\,1]) - E_{\mathrm{tot}}([1\,0\,0]) \tag{4}$$

The z axis we will always choose to be parallel to the normal of the film. Correspondingly, the x axis is always parallel to the plane of the film. In equation (4), E_{tot} is the total energy of the system.

In the case of Co and Fe films the calculations were performed for square lattices with lattice parameters 2.616 Å, and 2.729 Å. For the unsupported FePt film, two atomic layers of the $L1_0$ structure were considered with parameters ($a = 3.86$ Å, $c = 3.71$ Å). A typical $\mathbf{k}$ mesh size was 120×120 in the 2D Brillouin zone for the unit cells with two magnetic atoms.

[1] In equation (3) it is assumed that only the d states contribute significantly to the orbital moment. A general formula contains additionally the sum over quantum number l.

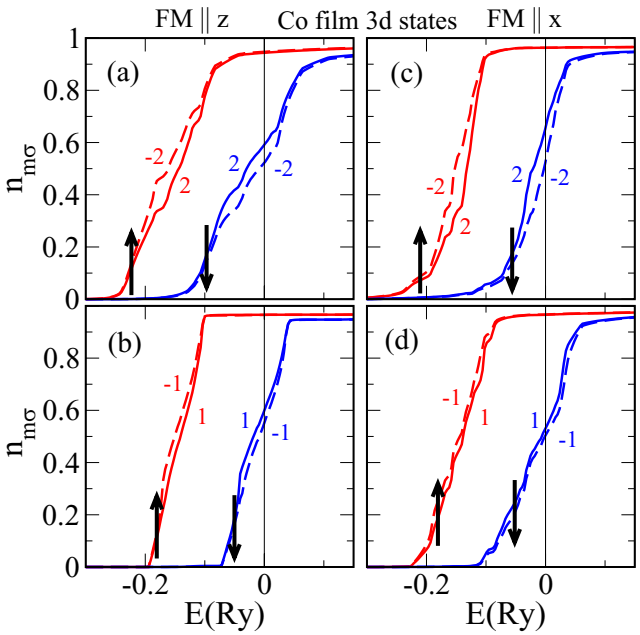

Figure 1. Energy dependence of the occupation numbers $n_{m\sigma}$ for 1ML Co film. The arrows show the spin projection, and the numbers give magnetic quantum number m. Panels (a) and (b) correspond to the ferromagnetic spin moments parallel to the z axis, panels (c) and (d) to the spin moments parallel to the x axis.

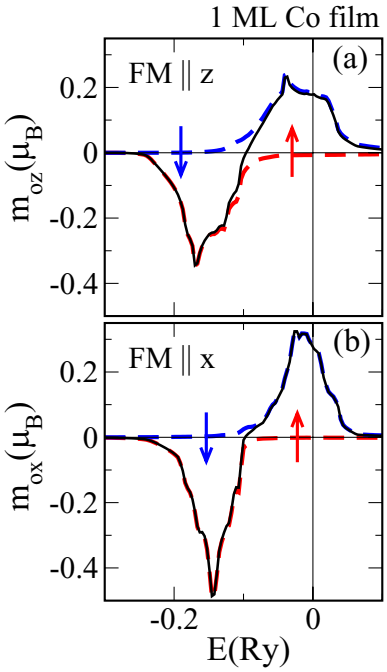

Figure 2. The atomic orbital moment of the 1ML Co film as the function of the upper energy of the band filling. (a) the ferromagnetic spin structure parallel to the z axis, (b) the ferromagnetic spin structure parallel to the x axis. The broken curves give the partial spin contributions, the solid curves present the total value of the orbital moment.

3. Collinear spin configurations

3.1. Formation of the orbital moment

3.1.1. 1ML Co and Fe films. The formation of the atomic orbital moments has substantial specific features in pure 3d elements and in the binary systems formed from both 3d and 4d/5d elements. We will start with the consideration of the Co film. In figure 1 we show the occupation numbers of the 3d orbitals with the given m and spin projection σ as a function of the upper energy of the band filling. $E = 0$ in the graph corresponds to the actual position of the Fermi level. The filling of the spin-up orbitals takes place at lower energies than the filling of the spin-down orbitals. This is the consequence of the spin splitting caused by the exchange interaction. In the absence of the SOC, $n_{-m} = n_m$ and the orbital moment is zero. The SOC lifts the degeneracy with respect to the sign of m resulting in the formation of the orbital moment. For the spin-up states the curve of the occupation of the negative-m orbitals lies above the corresponding positive-m curve (figure 1). This behaviour is anticipated since, for spin-up states, the on-site SOC term $\sigma_z \hat{l}_z$ tends to move the negative-m orbitals to lower energies and the positive-m orbitals to higher energies. For spin-down states the trend in the $\pm m$ splitting is opposite.

The orbital moment (equation (2)) as a function of the band filling is shown in figure 2. In agreement with $n_{m\sigma}$ dependences (figure 1) the filling of the spin-up orbitals gives a negative orbital moment, whose absolute value increases first, reaches a maximum, and starts to decrease. When all spin-up 3d orbitals are occupied, the corresponding contribution to the orbital moment becomes zero. The filling of the spin-down orbitals gives a positive orbital moment. As the spin-down orbitals are partially filled the compensation of the positive and negative m at the Fermi level ($E = 0$) does not take place and the system has a positive orbital moment in agreement with Hund's third rule.

Since the orbital moment results from the energy shifts of the electron states there is a relation between the orbital moment and the modification of the energy of the system due to the SOC. This is the physical basis of Bruno's formula [8]:

$$\mathrm{MAE} \approx -\frac{\xi}{4\mu_B}\mathrm{OMA} \tag{5}$$

The origin of the anisotropy of the orbital moment is seen from the analysis of the occupation numbers $n_{m\sigma}$ for the spin configurations parallel to the z and x axes (figure 1). The general structure of the curves shown in figures 1(a)–(d) is the same. However, in detail the curves are different. This is the result of the structural anisotropy of the system. Consequently, the curves of the orbital moment as a function of the upper filling energy are different (figure 2).

It is instructive to compare both quantities, MAE and OMA, as the functions of band filling (figure 3). In the small-n region of the initial filling of the spin up states, the signs of the MAE and OMA are expected to be the same, since here the orbitals with negative m are predominantly occupied. Indeed there is a clear similarity to the MAE and OMA curves in the interval of n between 0 and 4. In the region of the filling of the spin-down states (n above 6), MAE and OMA have opposite signs, as is reflected in Bruno's relation. In the intermediate region ($4 < n < 6$) the two curves have very different behaviour. By scaling the OMA curve we can get the gut coincidence of the MAE(n) and OMA(n) in the intervals

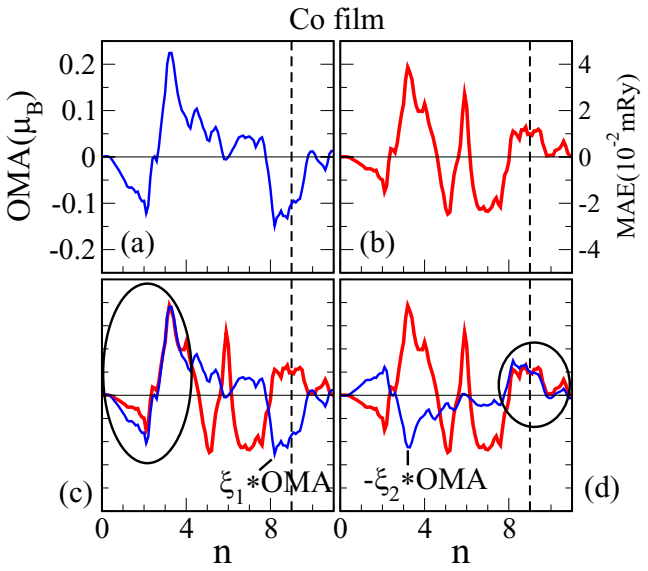

Figure 3. OMA and MAE of 1ML Co film as functions of the electron number. (*a*) OMA; (*b*) MAE; (*c*) comparison of the OMA and MAE curves. The OMA curve is scaled to reach the best agreement with the MAE curve in the low-n region; (*d*) comparison of the OMA and MAE curves. The OMA curve is scaled to reach the best agreement with the MAE curve in the large-n region. The ratio of the scaling parameters $\xi_1/\xi_2 = 1.7$.

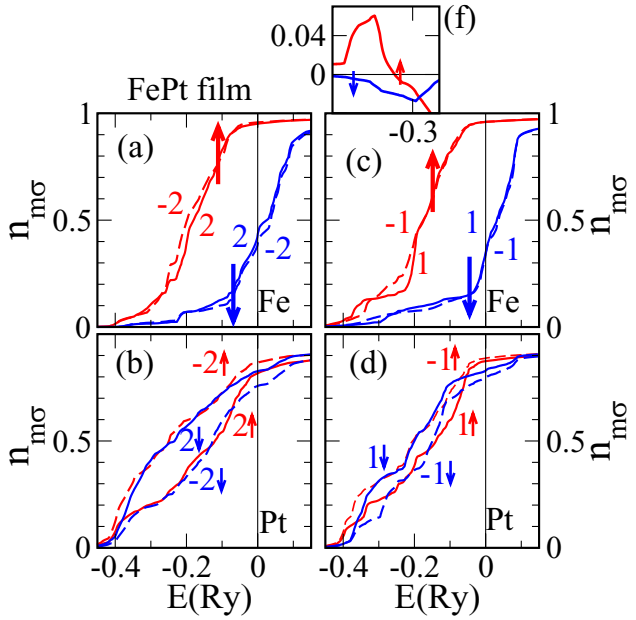

Figure 4. Energy dependence of the occupation numbers $n_{m\sigma}$ for Fe (panels (*a*) and (*c*)) and Pt (panels (*b*) and (*d*)) atoms in the 1ML FePt film. The ferromagnetic spin structure is parallel to the z axis. The arrows show the direction of the spin projection, and the numbers give the values of magnetic quantum number m. Panel (f) shows the differences ($n_{1\sigma} - n_{-1\sigma}$) for the spin-up and spin-down Fe orbitals in energy intervals from -0.35 Ry to -0.27 Ry.

of n from 0 to 4 (figure 3(*c*)) and from 8 to 10 (figure 3(*d*)). However, the scaling factor in the [0,4] interval is 1.7 times larger then in the [8,10] interval. This shows that the spatial derivative of the electronic potential contained in the first-principles formula of the SOC [25] acts with different effective strength in different parts of the electronic spectrum.

We performed similar calculations for the 1ML Fe film. The results for the Fe film are qualitatively similar to those shown in figures 1–3 for the Co film and we do not present them.

3.1.2. 1ML FePt film. Figure 4 shows the $n_{m\sigma}(E)$ dependencies for both the Fe and Pt atoms for the ferromagnetic spin configuration parallel to the z axis. The properties of the curves for the Fe atom in FePt are in many respects similar to the corresponding curves for the Co atom in the Co film (figure 1).

The important difference between the Pt 5d and Fe 3d dependencies is the weak spin splitting of the Pt 5d states. This splitting is much smaller than the width of the Pt 5d bands. As a result, the four curves in figures 4(*b*) and (*d*) are not separated in energy into two pairs as the Fe 3d states are, but form one bunch of four lines. The energy interval of the variation of the number of the d electrons from 0 to saturation spreads from about -0.4 Ry to about 0.05 Ry for both Fe and Pt. The common energy interval reflects the hybridization of the Fe 3d and Pt 5d states.

For the Fe 3d states the hybridization with the Pt states leads to an important effect absent in the pure Co and Fe films: The reversal of the relative positions of the $m = 1$ and $m = -1$ curves (figure 4(*c*)). This reversal takes place for both spin channels: For the spin-up states the $m = 1$ orbitals become more strongly occupied than the $m = -1$ orbitals, whereas for the spin-down states the $m = -1$ orbitals are more strongly occupied than the $m = 1$ orbitals. In figure 4(f) we show the occupation differences ($n_1 - n_{-1}$). Opposite to the trend governed by the on-site SOC and Hund's third rule, the spin-up difference curve has a positive sign and the spin-down curve has a negative sign. This is the result of the hybridization of the Fe 3d states with the $\pm m$ polarized Pt 5d states. Thus we deal with the $\pm m$ polarization of the Fe states induced by the SOC on the neighboring atoms, which cannot be described in terms of Hund's rule. The effect of the anomalous reversal of the occupations increases if we perform the calculation with the SOC present on the Pt site only (not shown). On the other hand, the effect disappears if only the Fe SOC is taken into account. This proves that the interatomic hybridization is the origin of the effect.

Also, in the dependence of the value of the orbital moment on the band filling we obtain anomalous behaviour (figure 5). For the spin-up Fe 3d orbitals in the spin structure parallel to the z axis (figure 5(*a*)), there are two energy regions where the contribution to the orbital moment is positive: From -0.41 Ry to -0.29 Ry and, from -0.12 Ry to -0.09 Ry. For the spin-down orbitals there is one anomalous energy interval from -0.4 Ry to -0.22 Ry. For the spin structure parallel to the x axis (figure 5(*c*)) the anomalies become even more developed.

The anisotropy of the anomalous behaviour is reflected in another remarkable feature of the $n_o(E)$ curve that is present only for the spin configuration parallel to the x axis. This is the local minimum of the spin-down contribution to the Fe orbital moment lying directly at the Fermi level (see figure 5(*c*) and insert in this figure). To reveal the origin of this feature we performed an analysis of the m and the spin resolved Fe 3d

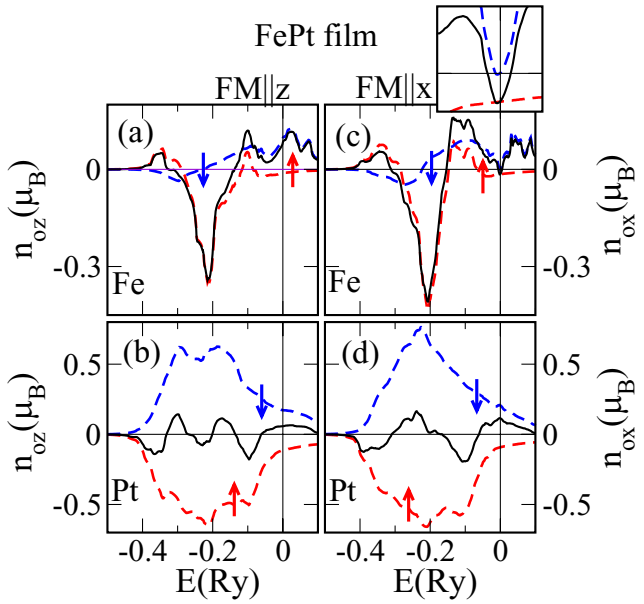

Figure 5. Orbital moments of Fe (panels (*a*) and (*c*)) and Pt (panels (*b*) and (*d*)) in a 1ML FePt film as functions of the upper filling energy. Panels (*a*) and (*b*) show the case of the ferromagnetic structure parallel to the *z* axis, panels (*c*) and (*d*) correspond to the ferromagnetic structure parallel to the *x* axis. The insert in panel (*c*) zooms in on the Fermi-energy region. The shown intervals are (−0.03 Ry, 0.02 Ry) for the abscissa axis and (−0.02 μ_B, 0.035 μ_B) for the ordinate axis. The broken curves show partial spin contributions. The arrows give the direction of the spin projection. The solid curves show the total value of the orbital moment.

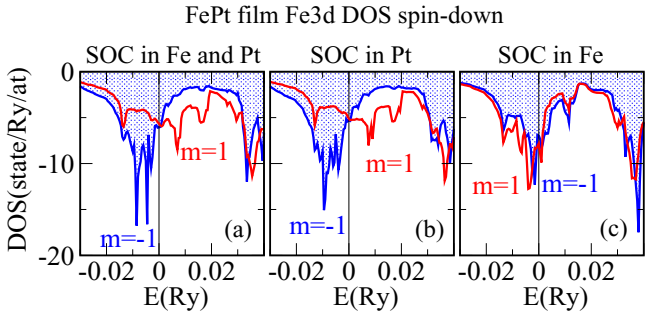

Figure 6. The spin-down Fe 3d DOS for $m = -1$ and $m = 1$. As is commonly adopted, the spin-down DOS is shown below the abscissa axis. (*a*) SOC in both Fe and Pt; (*b*) SOC in Pt atoms only; (*c*) SOC in Fe atoms only.

density of states (DOS). For the spin structure parallel to the *x* axis we indeed found an anomalous behaviour of the DOS in the region of the Fermi energy (figure 6) consisting of a sharp dominating peak of $m = -1$ DOS located just below the Fermi energy E_F, followed by the energy region above E_F with a dominating $m = 1$ DOS. We characterize this feature as an anomaly in the same sense as above in order to emphasize that it cannot originate in the on-site Fe SOC. If the SOC in the Fe atoms is switched off, the properties of the DOS change weakly (figure 6(*b*)). On the other hand if the Pt SOC is switched off the anomaly disappears (figure 6(*c*)).

3.2. Rotation of the collinear magnetic configuration

3.2.1. Co and Fe films. Next we consider the properties of the Co and Fe films with the ferromagnetic spin moments

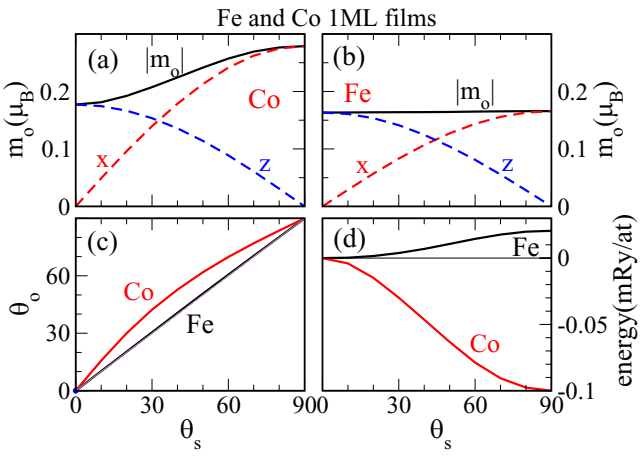

Figure 7. The θ_s dependence of the calculated quantities for Fe and Co films. (*a*) Components and modulus of the Co orbital moment; (*b*) components and modulus of the Fe orbital moment; (*c*) angle θ_o giving the direction of the orbital moments for both films; (*d*) energy for both films.

assuming the directions that are intermediate between the *z* and *x* axes. The direction of the spins is specified by the angle θ_s counted clockwise from the *z* axis. Figure 7 shows the θ_s dependencies of the components and the modulus of the orbital moment of the Co (panel (*a*)) and Fe (panel (*b*)) atoms, of the direction of the orbital moment θ_o (panel (*c*)) and of the energy (panel (*d*)).

We notice that the θ_s dependence of the projections of the orbital moment (figure 7(*a*)) is well-described by simple expressions:

$$m_{ox}(\theta_s) = M_{ox}\sin(\theta_s), \quad m_{oz}(\theta_s) = M_{oz}\cos(\theta_s).$$

In the case of Co, the amplitudes M_{ox},M_{oz} are different. This difference determines the OMA. In the case of Fe the OMA is weak. The anisotropy of the orbital moment correlates with the non-collinearity of the spin and orbital moments (figure 7(*c*)) as discussed in [24].

The absolute value of the spin moment depends weakly on θ_s and the spin projections are well-described by the expressions:

$$m_{sx}(\theta_s) = M_s\sin(\theta_s), \quad m_{sz}(\theta_s) = M_s\cos(\theta_s).$$

This is a common property of the spin moments in the collinear spin configurations of all the systems studied. The simple functional form of the projections of both the spin and orbital moments as functions of θ_s leads to the θ_s-independent ratios m_{ox}/m_{sx} and m_{oz}/m_{sz}. In section 4.2.1 we will compare the ratios for different systems.

3.2.2. FePt film. In figure 8 we show the calculated θ_s dependence of the properties of the FePt film. In sharp contrast to the Co and Fe films we obtained a negative m_{ox} projection of the Fe orbital moment for all the values of θ_s. Besides the difference in sign, the curve $m_{ox}(\theta_s)$ is also different in shape, strongly deviating from a simple sine function. Above $\theta_s \sim 50^\circ$ the value of m_{ox} of Fe becomes almost independent

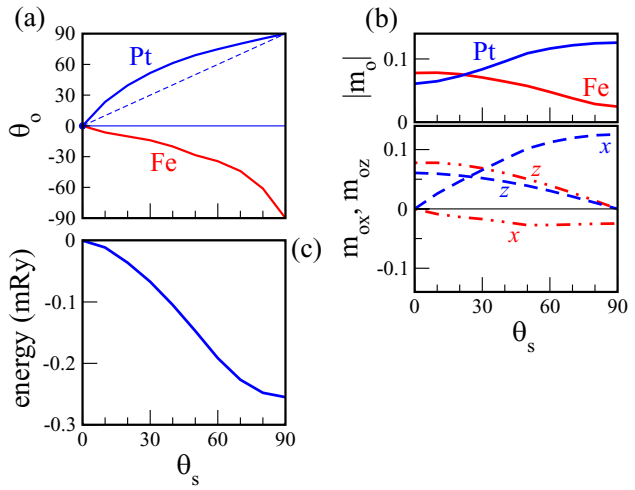

Figure 8. The θ_s dependence of the calculated quantities for the FePt film. (a) angle θ_o gives the directions of the orbital moments of the Fe and Pt atoms, the dashed, sloping straight line shows the line $\theta_o = \theta_s$; (b) components and absolute values of the Fe and Pt orbital moments; (c) energy.

of θ_s. This leads to a very peculiar θ_s-dependence of the ratio m_{ox}/m_{sx}, which is very different from the θ_s-independent ratio m_{oz}/m_{sz} of the z projections (see figure 18(a)). Therefore, even for simple collinear configurations, the behaviour of the ratio of the projections of the atomic orbital and spin moments can be highly non-trivial.

The negative m_{ox} projection leads to the property that the angle between the spin and orbital moments of the Fe atoms increases continuously from 0° for a spin moment parallel to the z axis, $\theta_s = 0°$, to 180° for a spin moment parallel to the x axis, $\theta_s = 90°$ (figure 8(a)). For the intermediate θ_s values, the inducing spin moment and the induced orbital moment become orthogonal to each other. Obviously, all the peculiar properties of the x projection are related to each other and have the same physical origin: The influence of the Pt SOC. Below we will show that for non-collinear spin configurations the properties of the Fe orbital moments in a FePt film become even more spectacular.

4. Noncollinear magnetic configurations

To introduce non-collinear spin configurations we double the volume of the unit cell compared to the calculations for the collinear spin configurations reported above. Then we study the SOC-governed properties as a function of the angle between two atomic spins in the increased unit cell. The non-collinear configurations are characterized by two angles: θ_{net} and θ_{inter}. θ_{net} gives the direction of the net spin magnetization, θ_{inter} is the angle between the two atomic spins (figure 9). To study the anisotropy properties for a given non-collinear spin configuration we vary θ_{net}, keeping θ_{inter} fixed. To study the trends related to the increasing angle between spin moments we consider different θ_{inter}.

4.1. Variation θ_{net} for fixed θ_{inter}

As above, we begin with the consideration of the Co film. The calculations for the non-collinear spin configurations with

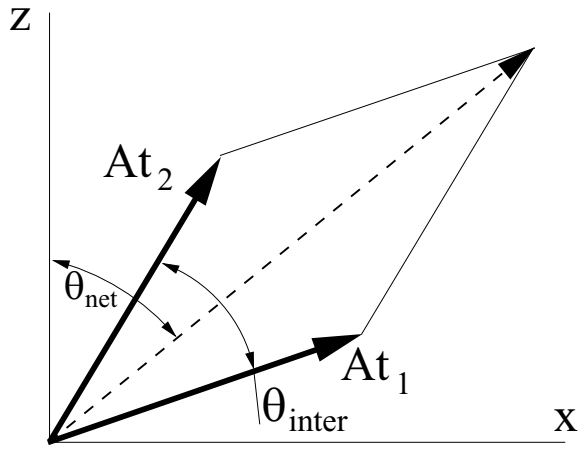

Figure 9. Definition of the first and second atoms and the angles θ_{net} and θ_{inter} in the non-collinear spin configurations.

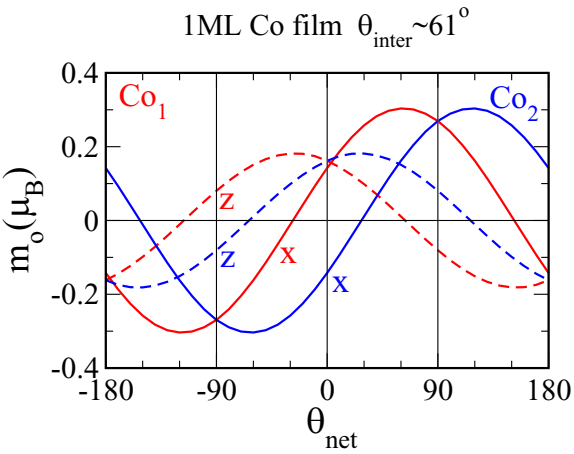

Figure 10. The projections of the orbital moments of two Co atoms in a 1ML Co film as a function of the θ_{net} angle. The angle between the spins of the atoms θ_{inter} has a fixed value of ~61°. The broken lines show the z projections, the solid lines show the x projections. The red curves correspond to Co_1 and the blue curves correspond to Co_2.

a given θ_{inter} give weak dependence of the spin moments on θ_{net}. In figure 10 we show the calculated projections of the orbital moments for $\theta_{\text{inter}} \sim 61°$. The disadvantage of the plot of the projections as a function of θ_{net} is the fact that θ_{net}, as an average angle, does not give the directions of the spin moments of individual atoms. This complicates the comparison of the curves obtained for different θ_{inter} and the conclusions about relative directions of the atomic spin and orbital moments. It is convenient to redraw the figure using the spin directions θ_s of the atomic moments as the abscissa variable. This is done in figure 11(a), which was obtained from figure 10 by the shift of the projections of the orbital moment of Co_1 to the right by $\theta_{\text{inter}}/2$ and of the projections of Co_2 to the left by the same value. After these shifts the curves of both atoms practically coincide with each other and are very close to the corresponding curves for the collinear Co configuration (figure 7). This means that the Co-orbital moments in the non-collinear configuration depend weakly on the spin configuration of the neighboring atoms and are largely

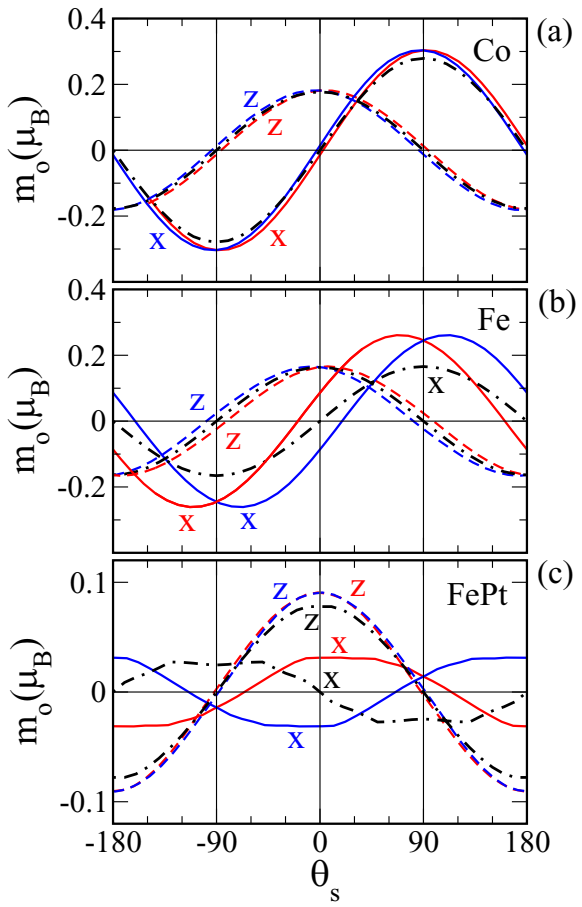

Figure 11. Projections of the orbital moments as functions of θ_s. (a) Co film. The angle between spins of the atoms θ_{inter} has a fixed value of $\sim 61^\circ$. The curves are obtained from those presented in figure 10 by the shift along the abscissa axis. The black dashed–dotted curves show the θ_s dependences of the orbital moment projections for the collinear ferromagnetic structure. (b) The same as in panel (a) but for the Fe film. The angle between the spin moments of the Fe_1 and Fe_2 atoms is $\sim 74^\circ$. (c) The same as in panels (a) and (b) but for the Fe atoms in the FePt film. The angle between the spin moments of the Fe_1 and Fe_2 atoms is $\sim 76^\circ$.

determined by the direction of the corresponding atomic spin with respect to the atomic lattice. This result can be considered as a basis for the treatment of the magnetic anisotropy of a system in terms of single-site anisotropy with a temperature-independent anisotropy constant. Such an assumption is often used in model-Hamiltonian studies. As is shown below, other considered systems do not favor such simplified treatment.

Figure 11(b) shows the results of the calculations for the Fe film. The difference with the corresponding curves for the Co film is clearly seen. If the z components for both the Fe atoms are rather close to each other and similar to the curve obtained for the ferromagnetic configuration, the x projections are strongly shifted with respect to each other and have a much larger amplitude than the amplitude of $m_{ox}(\theta_s)$ obtained for the collinear spin configuration (figure 7). The relative shift of the x projections means that the direction of the orbital moment of a given Fe atom depends on the orientations of the spins of the neighboring atoms. The increased amplitude of the x component compared to the collinear configuration suggests

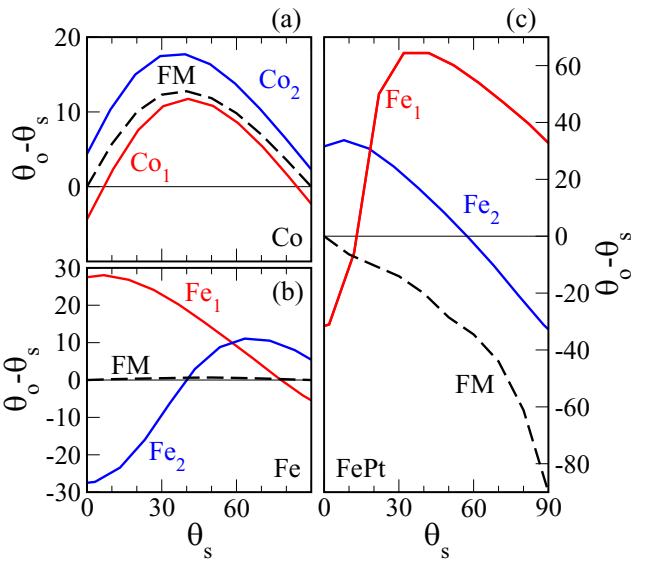

Figure 12. Angle between atomic orbital and spin moments $\theta_o - \theta_s$ as a function of the direction of the spin moment. (a) Co film. The angle θ_{inter} between the spins of the Co_1 and Co_a atoms has a fixed value of $\sim 61^\circ$. A black dashed-dotted curve shows the $\theta_o - \theta_s$ for the collinear ferromagnetic structure. (b) The same as in panel (a) but for the Fe film. The angle between the spin moments of the Fe_1 and Fe_2 atoms is $\sim 74^\circ$. (c) The same as in panels (a) and (b) but for the Fe atoms in the FePt film. The angle between the spin moments of the Fe_1 and Fe_2 atoms is $\sim 76^\circ$.

that the change in the electronic structure, that is caused by the non-collinearity of the spins, has an important influence on the absolute value of the orbital moment.

Also, in the case of FePt we obtained a strong difference in the properties of the z and x projections of the orbital moments (figure 11(c)). If $m_{oz}(\theta_s)$ functions for both the Fe atoms are close to each other and to the one for the ferromagnetic configuration, the three $m_{ox}(\theta_s)$ curves are greatly different from each other.

The different behaviour of the projections of the orbital moments presented in figure 11 results in different properties of the angles between the spin and orbital moments for the three systems. These angles are accessible in modern experiments and the theoretical demonstration of their different behaviour in different systems should be the motivation for the corresponding experimental studies. In figure 12 we show $\theta_o - \theta_s$ as a function of θ_s for the two atoms in the non-collinear configurations and for the atom in the ferromagnetic structure. In the case of Co (figure 12(a)), all three curves are rather similar, which shows again that for this system the non-collinearity of the magnetic structure leads to a moderate influence on the relative directions of the atomic spin and orbital moments. For the Fe film the difference between the three curves is large (figure 12(b)). Here the maximal deviation of the orbital moment from the spin moment is obtained for θ_s that is close to zero. This means that when the spin of the atom is parallel to the z axis the orbital moment deviates by an angle of $\sim 28^\circ$. For the collinear ferromagnetic configuration, by symmetry, $\theta_o - \theta_s = 0^\circ$ for $\theta_s = 0^\circ$.

In FePt, the properties of $\theta_o - \theta_s$ become even more peculiar (figure 12(c)). When a spin moment of Fe_1 is parallel

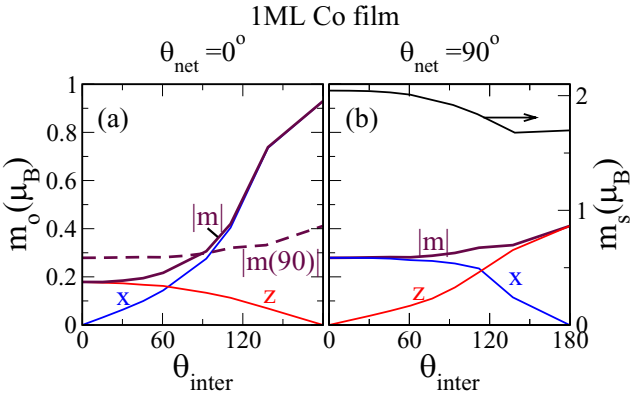

Figure 13. The dependence of the Co spin and orbital moments in the 1ML Co film on the angle θ_{inter}. (a) Calculations for $\theta_{\text{net}} = 0$; (b) calculations for $\theta_{\text{net}} = 90^\circ$. The spin moment as a function of θ_{inter} is presented only once in panel (b). The x and y projections of the orbital moment are labelled x and y; $|m|$ labels the absolute value of the orbital moment. The dashed line labelled |m(90)| in panel (a) copies the modulus line from panel (b).

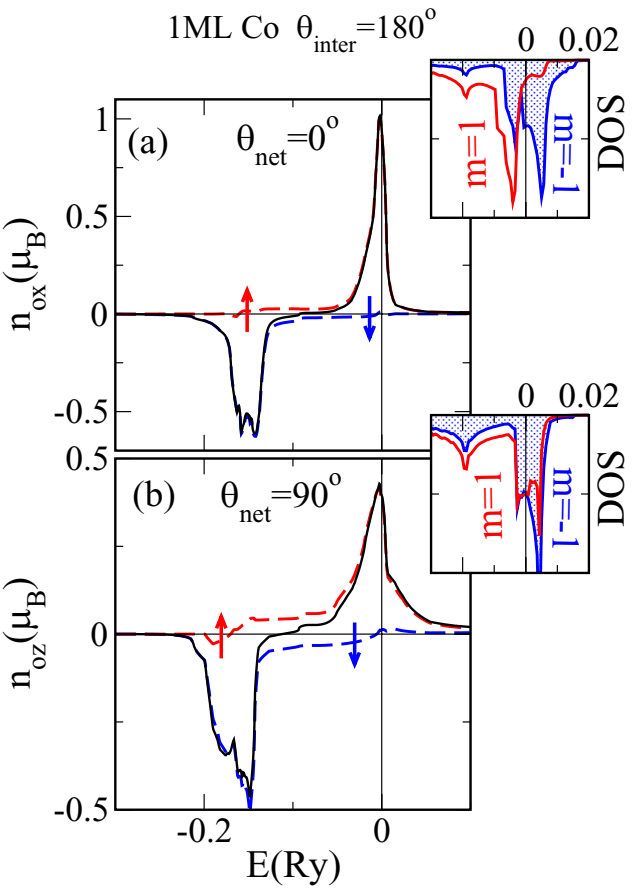

Figure 14. Projections of the Co orbital moment in 1ML Co film for the anti ferromagnetic configuration of the spin moments. (a) $\theta_{\text{net}} = 0^\circ$; ($b$) $\theta_{\text{net}} = 90^\circ$. The dashed curves show partial spin contributions, the solid curves show the total value of the orbital moment. In the inserts are the fragments of the DOS for $|m| = 1$, demonstrating the reason for the formation of an enhanced orbital moment.

to the z axis ($\theta_s = 0^\circ$), its orbital moment deviates to the left by a large angle of about 30°. With increasing θ_s the angle between the two atomic moments quickly decreases. At $\theta_s \sim 13^\circ$ the moments become parallel. With a further increase of θ_s, the orbital moment deviates to the right from the spin moment, reaching a maximum of ∼60° at $\theta_s \sim 32^\circ$ and monotonously decreasing to ∼30° at $\theta_s = 90^\circ$. The orbital moment of the Fe_2 atom at $\theta_s = 0^\circ$ deviates from the spin moment to the right by ∼30°. This deviation first increases slightly and then monotonously decreases, changing sign and reaching a negative value of about -30° at $\theta_s = 90^\circ$. Both the curves obtained for the non-collinear structure are principally different from the curve obtained for the ferromagnetic configuration.

4.2. Variation of the angle between spin moments

To reduce the amount of graphical materials we will present the θ_{inter} dependencies only for $\theta_{\text{net}} = 0^\circ$ and $\theta_{\text{net}} = 90^\circ$. One advantage of these θ_{net} values is an increased symmetry of the system, leading to the equivalence of the two 3d atoms. In figure 13, we show the dependence of the Co spin and orbital moments on θ_{inter}. Since the value of the spin moment depends very weakly on θ_{net}, we present its value only in panel (b). For $\theta_{\text{net}} = 0^\circ$ (panel (a)) the dependence of the z projection of the orbital moment is well described by a simple cosine function. However, the functional dependence of m_{ox} deviates far from a simple sine form. With increasing θ_{inter} the x projection strongly increases, reaching at $\theta_{\text{inter}} = 180^\circ$ a large value of 0.93 μ_B to be compared to a moderate value of 0.18 μ_B at $\theta_{\text{inter}} = 0^\circ$.

It is instructive to discuss the origin of the obtained strong enhancement of the atomic orbital moment. The calculations of the electronic structure for the configuration with $\theta_{\text{inter}} = 180^\circ$ show a strong narrowing of the 3d bands compared to the ferromagnetic structure with $\theta_{\text{net}} = 0^\circ$ (not shown). We remark that the narrowing of the electron bands in an excited ferromagnet was detected in a pump-probe experiment [27]. Since the narrow bands lay close to the Fermi energy, the SOC can lead to a stronger imbalance between the occupation of the m and $-m$ orbitals than for configurations with a small θ_{inter}. As shown in figure 14(a), this is exactly what happens in the case of the configuration with $\theta_{\text{inter}} = 180^\circ$ and $\theta_{\text{net}} = 0^\circ$. The SOC leads to the splitting of the peak of the states with $m = 1$ and $m = -1$ into two separate peaks. The peak with $m = 1$ is almost completely occupied, whereas the peak with $m = -1$ is almost empty. This strong $\pm m$ polarization results in a large orbital moment.

For $\theta_{\text{net}} = 90^\circ$, the increase in the magnitude of the orbital moment with an increase in θ_{inter} is much weaker. This is explained by the stronger hybridization of the m and $-m$ orbitals, resulting in a smaller effect of the SOC.

In figure 15 we compare the θ_{inter} dependences of the OMA and MAE for the Co and Fe films. There are a number of important differences between the two systems. First, for the Co film the OMA and MAE dependences can be scaled to coincide within a wide θ_{inter} interval. This supports the applicability of the Bruno picture for magnetically excited states. For Fe this is not possible since the small negative OMA value for the ferromagnetic configuration ($\theta_{\text{inter}} = 0^\circ$ in

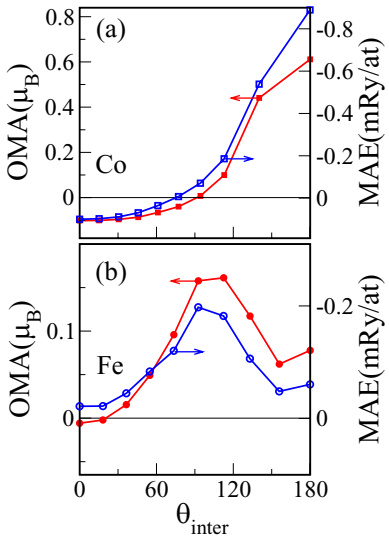

Figure 15. The OMA and MAE as functions of θ_{inter} for a 1ML Co film (panel (*a*)) and a 1ML Fe film (panel (*b*)).

figure 15(*b*)) does not correspond in sign to the MAE value. Second, the derivatives of the MAE as a function of θ_{inter} in the region of small θ_{inter} have the same sing for both Co and Fe. However, the initial MAE values are of the opposite sign. As the result, in Co the MAE decreases with increasing θ_{inter}, whereas in Fe it increases. This result is in direct correlation with the observation of different temperature trends in the variation of the MAE.

Turning to the discussion of the FePt film we notice that the Fe spin moment remains practically unchanged with the variation from the ferromagnetic spin configuration $\theta_{inter} = 0^\circ$ to the anti ferromagnetic spin configuration $\theta_{inter} = 180^\circ$ (see figure 16(*a*)). On the other hand, the induced Pt spin moment decreases monotonously with increasing θ_{inter}. The behaviour of the orbital moments is very different. On the basis of the study of the collinear configurations we expect the competition of the influences of the Fe SOC and Pt SOC. Since the Pt spin moment decreases with increasing θ_{inter}, the influence of the Pt SOC should also decrease. The details of the competition depend on the value of θ_{net}.

For $\theta_{net} = 0^\circ$ the absolute values of both the Fe and Pt orbital moments decrease with increasing θ_{inter} (figures 16(*b*) and (*c*)). In this case the SOC in Fe has a stronger impact than the SOC in Pt: First, in the main part of the interval of the θ_{inter} variation the absolute value of the Fe orbital moment is larger than the absolute value of the Pt orbital moment and, second, the x projection of the Fe moment is positive and corresponds to the sign expected on the basis of Hund's 3rd rule, whereas the sign of the x projection of the Pt orbital moment is negative and must be induced by the Fe SOC.

For $\theta_{net} = 90^\circ$ (figures 16(*d*) and (*e*)), at small θ_{inter} the SOC of Pt clearly wins the competition. At $\theta_{inter} = 0^\circ$, the value of the Pt orbital moment is much larger than the value of the Fe orbital moment. The negative value of the x projection of the Fe orbital moment reveals that the contribution coming through the hybridization with the Pt states is larger than the contribution of the on-site Fe SOC. With increasing θ_{inter} the

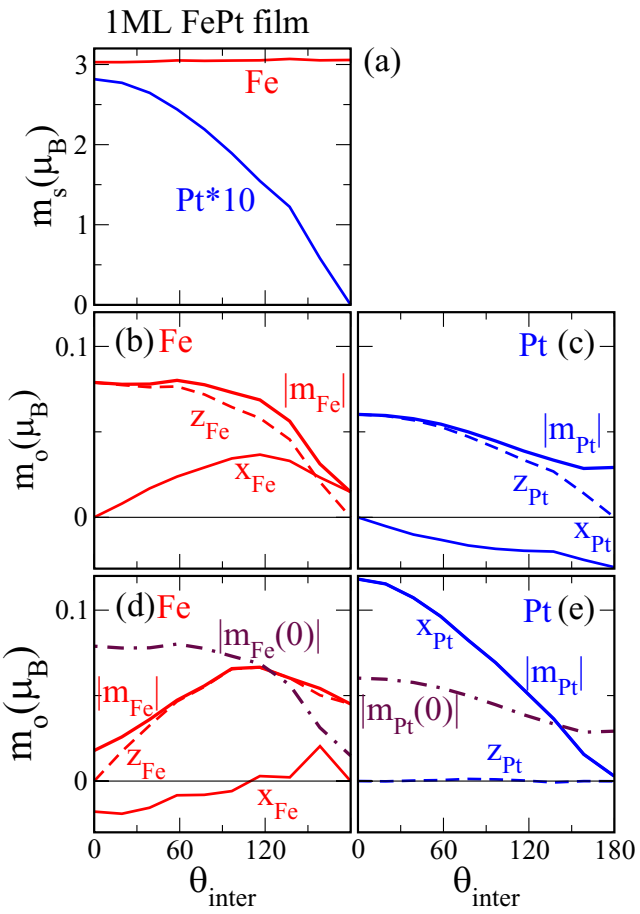

Figure 16. The dependence of the spin and orbital moments of Fe and Pt in a 1ML FePt film on the angle θ_{inter}. (*a*) Spin moments, Pt moments are multiplied by factor 10; (*b*) Fe, calculation for $\theta_{net} = 0$; (*c*) Pt, calculation for $\theta_{net} = 0$; (*d*) Fe, calculation for $\theta_{net} = 90^\circ$; (*e*) Pt, calculation for $\theta_{net} = 90^\circ$. The projections of the orbital moment are labelled with x_{At} and y_{At}, where At is either Fe or Pt; $|m_{At}|$ labels the absolute value of the orbital moment. The dotted–dashed line in panel (*d*) labelled $|m_{Fe}(0)|$ copies the modulus line from panel (*b*). The dotted-dashed line in panel (*e*) labelled $|m_{Pt}(0)|$ copies the modulus line from panel (*c*). The comparison of the $|m_{At}|$ and $|m_{At}(0)|$ lines gives the dependence of the OMA on θ_{inter}.

negative x component of the Fe moment decreases in absolute value and changes sign at θ_{inter} of about 110°. Thus, there is a clear trend of the transition from the leading role of the Pt orbital magnetism at $\theta_{inter} = 0^\circ$ to the opposite for larger θ_{inter}.

The OMA for Fe and Pt is determined by the differences in the pairs of the curves labelled $|m_{At}(0)|$ and $|m_{At}|$ in figures 16(*d*) and (*e*). Here, At is either Fe or Pt. These differences are presented in figure 17(*a*). Both functions are monotonous in the whole interval of the variation of θ_{inter}. They decrease in absolute value with an increasing θ_{inter}, cross the abscissa axis, and increase in absolute value again. The functions are, however, opposite in sign. The MAE as a function of θ_{inter} is presented in figure 17(*b*). It is positive at a small θ_{inter}, changes sign at about 90°, goes through a minimum, and increases again. This non-monotonous behaviour reflects the changes in the competition between the SOC Fe and SOC Pt. At the beginning of the θ_{inter} interval, the sign of the MAE corresponds to the sign

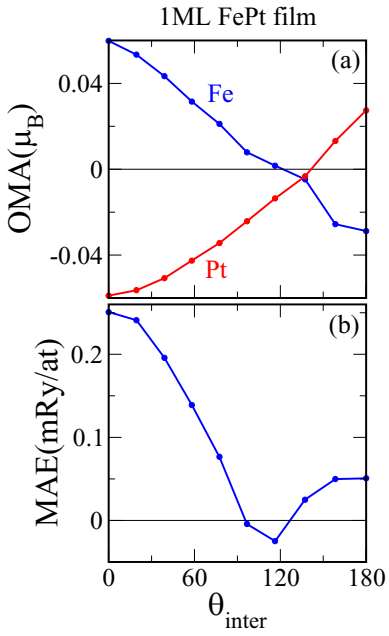

Figure 17. (*a*) The OMA of Fe and Pt atoms in 1ML FePt film as a function of θ_{inter}. (*b*) The MAE of the 1ML FePt film as a function of θ_{inter}.

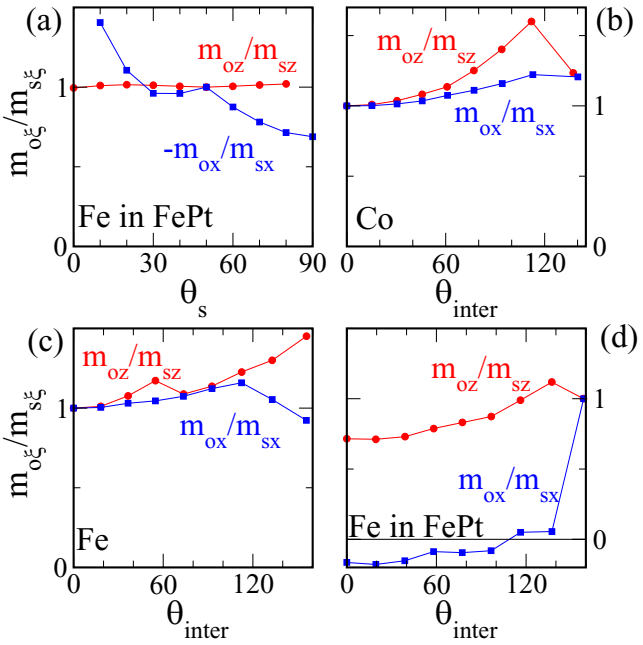

Figure 18. The angular dependence of the ratios of the components of the orbital and spin moments. (*a*) Dependence on θ_s for Fe atoms in the FePt film. The spin configuration is ferromagnetic. (*b*) Dependence on θ_{inter} for Co atoms in the Co film. (*c*) Dependence on θ_{inter} for Fe atoms in the Fe film. (*d*) Dependence on θ_{inter} for Fe atoms in the FePt film. All the curves are scaled to facilitate the comparison.

of the OMA of Pt; at the end of the interval it corresponds to the sign of the OMA of Fe. The violation of the simple relation (equation (5)) between the MAE and OMA due to the interatomic hybridization was first reported by Anderson *et al* [28] in their study of Au/Co/Au trilayers.

4.2.1. Ratio of the components of the orbital and spin moments. As mentioned in the Introduction, the modern methods of XMCDS provide element-specific information on the projections of atomic spin and orbital moments. The experimental studies have shown that the ratio of the components of the orbital and spin moments of a given type of atom can both remain almost unchanged and vary strongly in their magnetically excited states. Boeglin *et al* [6] obtained a considerable variation of the ratio and suggested treating this property as a signature of the separate dynamics of the spin and orbital moments. Figure 18 shows the dependences for the systems studied in this paper that show a strong variation in behaviour. Therefore, the variation of the ratio of the orbital and spin moments does not give a basis for the treatment of the orbital moment as a separate degree of freedom. The change in spin structure leads to the modification of the electronic structure, and as a result to a change in the orbital moments that, in general, has a complex non-trivial form and does not conserve the ratio of the components of the moments.

5. Conclusions

The presently available experimental data on the SOC-governed properties provide a rich and controversial picture. Thus, the magnetic anisotropy energy, depending on the material, can both increase and decrease, although the expected behaviour is a decrease. Also, the ratio of the projections of the spin and orbital moments measured as a function of temperature in slowly heated systems, or as a function of time in laser irradiated systems, changes, depending on the material, from almost constant to varying strongly. This variety of properties cannot be understood without a profound knowledge of the relation between spin and orbital magnetism in excited states of magnetic materials.

In this paper we report the first-principles study of the relation between spin and orbital magnetism in 1ML films of Co, Fe and FePt. We consider two types of perturbation of the ground-state spin structure. First, the collinear spin structure is continuously rotated between the easy and hard magnetization axes. Second, the collinear ground-state structure is replaced by non-collinear spin configurations with different angles between the atomic spin moments and the different directions of the net magnetization. In all the cases we calculate the directions and values of the atomic orbital moments, the magnetic anisotropy energy, the ratio of the projections of the spin and orbital moments, and relate them to the corresponding spin structure.

One important result from our study is the diversity of the obtained behaviour. In correlation with the experiment, we found that the dependence of the magnetic anisotropy and the ratio of the projections of the spin and orbital moments on spin disordering are principally different in different systems. We trace the origin of the diversity of properties to the characteristics of the electronic structure. Some calculated features are common for all the systems studied. For instance, the on-site SOC in the magnetic atoms produces a trend to the earlier filling of the atomic spin-up orbitals with negative magnetic

quantum numbers m compared to the orbitals with positive m. For the spin-down orbitals the trend is the opposite. This trend is closely connected with Hund's 3rd rule and Bruno's model suggesting a simple relation between OMA and MAE. On the other hand the influence of the SOC on the neighboring atoms transferred through interatomic hybridization varies strongly from material to material and is the origin of various anomalies such as violation of Hund's 3rd rule and the failure of Bruno's model. Our study of the magnetic anisotropy shows that the concept of temperature independent magnetic anisotropy constants fails in many systems.

One important aspect of spin-disordering is the change in electronic structure. Since the spin non-collinearity directly influences the exchange interactions in the systems, the change in electronic structure is stronger than the influence of the SOC and cannot be neglected. In particular, we obtained a trend of the narrowing of the energy bands in the region of the Fermi energy. This result correlates with the experimental observation of the band narrowing in a laser irradiated system.

Despite the importance of the temperature dependence of the magnetic anisotropy for both fundamental physics and applications, little is being done in this direction within the framework of the first-principles calculations. A rare exception is the work by Staunton *et al* [18, 29, 30]. It is worth relating this work to the approach used in this paper. The disordered local moment (DLM) method employed by Staunton *et al* uses the directions of the atomic spin moments as independent variables and performs statistical mechanics averaging over the ensemble of non-collinear spin configurations. The calculations are based on the single-cite coherent potential approximation (CPA) approach that reduces to the determination of the probability function for the direction of a selected atomic spin in an effective-medium environment. The probability function and the parameters of the effective medium are temperature dependent. The application of this method provided a number of interesting results such as a non-trivial power dependence of the magnetic anisotropy energy of bulk FePt and FePd as a function of the average magnetization [18, 29] and a non-monotonous temperature dependence of the magnetic anisotropy of the Co films on Cu(1 0 0) [30]. Although the calculations by Staunton *et al* are fully relativistic and include in principle the orbital magnetism, the orbital moments were not evaluated. The single-site approximation in the averaging procedure is a rather strong simplification of the physical picture, whose influence on the quantitative accuracy of the calculated physical properties is not easy to estimate. In this respect, the single-site CPA method used by Staunton *et al* and the approach used in this paper can be considered as complementary. Combining the properties of both approaches within one calculational scheme would be an advantage. Thus, the consideration of non-local effects within the non-local CPA approach [31] can provide a better account for the properties of individual spin configurations. On the other hand, the increase in the number of the non-collinear spin configurations studied and the statistical-mechanics averaging over them is one way of making the qualitative study in this work more quantitative. We hope that the present work will stimulate further advances in the first-principles studies of the magnetic anisotropy in systems disturbed from the ground state.

In general, we demonstrate that the response of the orbital moments on the excitation of the spin structure can vary from the rather simple and anticipated, to the very complex and unexpected. We show that behind this variety of behaviour lies a complex interplay of the properties of the electronic structure that cannot be revealed without detailed first-principles calculations.

References

[1] Gambardella P *et al* 2003 *Science* **300** 1130
[2] Xu Y B, Tselepi M, Guertler C M, Vaz C A F, Wastlbauer G and Bland J A C 2001 *J. Appl. Phys.* **89** 7156
[3] Cabria I, Nonas B, Zeller R and Dederichs P H 2002 *Phys. Rev.* B **65** 054414
[4] Thole B T, Carra P, Sette F and van der Laan G 1992 *Phys. Rev. Lett.* **68** 1943
[5] Dürr H A, Guo G Y, van der Laan G, Lee J, Lauhoff G and Bland J A C 1997 *Science* **277** 213
[6] Boeglin C, Beaurepaire E, Halte V, Lopez-Flores V, Stamm C, Pontius N, Dürr H A and Bigot J-Y 2010 *Nature* **465** 458
[7] Carpene E, Mancini E, Dallera C, Brenna M, Puppin E and De Silvestri S 2008 *Phys. Rev.* **B 78** 174422
[8] Bruno P 1989 *Phys. Rev.* B **39** 865
[9] Daalderop G H O, Kelly P J and Schuurmans M F H 1990 *Phys. Rev.* B **42** 7270
[10] Szunyogh L, Ujfalussy B, Blaas C, Pustogowa U, Sommers C and Weinberger P 1997 *Phys. Rev.* B **56** 14036
[11] Shick A B and Mryasov O N 2003 *Phys. Rev.* B **67** 172407
[12] Oppeneer P 1998 *J. Magn. Magn. Mater.* **188** 275
[13] Ravindran P, Kjekshus A, Fjellvaag H, James P, Nordström L, Johansson B and Eriksson O 2001 *Phys. Rev.* B **63** 144409
[14] Galanakis I, Alouani M and Dreysse H 2000 *Phys. Rev.* B **62** 6475
[15] Farle M, Platow W, Kosubek E and Baberschke K 1999 *Surf. Sci.* **439** 146
[16] Baberschke K 2001 *Band-Ferromagnetism: Ground-State and Finite-Temperature Phenomena* (*Lecture Notes in Physics* vol 580) (Berlin: Springer) pp 27–45
[17] Skomski R, Kashyap A, Solanki A, Enders A and Sellmyer D J 2010 *J. Appl. Phys.* **107** 09A735
[18] Staunton J B, Ostanin S, Razee S S A, Gyorffy B L, Szunyogh L, Ginatempo B and Bruno E 2004 *Phys. Rev. Lett.* **93** 257204
[19] Callen H B and Callen E 1966 *J. Phys. Chem. Solids* **27** 1271
[20] Tseng Y-C, Souza-Neto N M, Haskel D, Gich M, Frontera C, Roig A, van Veenendaal M and Nogues J 2009 *Phys. Rev.* B **79** 094404
[21] Stamm C *et al* 2008 *Phys. Rev.* B **77** 184401
[22] Bartelt A F, Comin A, Feng J, Nasiatka J R, Eimüller T, Ludescher B, Schütz G, Padmore H A, Young A T and Scholl A 2007 *Appl. Phys. Lett.* **90** 162503
[23] Herrero-Albillos J, Garca L M, Bartolome F and Young A T 2011 *Eur. Phys. Lett.* **93** 17006
[24] Sandratskii L M 2013 *Phys. Rev.* B **88** 064415
[25] Sandratskii L M 1998 *Adv. Phys.* **47** 91
[26] von Barth U and Hedin L 1972 *J. Phys.* C **5** 1629
[27] Stamm C *et al* 2007 *Nat. Mater.* **6** 740
[28] Andersson C, Sanyal B, Eriksson O, Nordström L, Karis O, Arvanitis D, Konishi T, Holub-Krappe E and Dunn J H 2007 *Phys. Rev. Lett.* **99** 177207
[29] Staunton J B, Szunyogh L, Buruzs A, Gyorffy B L, Ostanin S and Uvardi L 2006 *Phys. Rev.* **74** 144411
[30] Buruzs A, Weinberger P, Szunyogh L, Uvardi L, Chleboun P I, Fisher A M and Staunton J B 2007 *Phys. Rev.* **76** 064417
[31] Rowlands D A, Staunton J B and Gyorffy B L 2003 *Phys. Rev.* **67** 115109